Controllable g5p-Protein-Directed Aggregation of ssDNA−Gold Nanoparticles

Soo-Kwan Lee,[†] Mathew M. Maye,[†] Yian-Biao Zhang,[‡] Oleg Gang,[†] and Daniel van der Lelie*,[‡]

Center for Functional Nanomaterials, and Biology Department, Brookhaven National Laboratory, Upton, New York 11973

Received October 29, 2008. Revised Manuscript Received November 24, 2008

We assembled single-stranded DNA (ssDNA) conjugated nanoparticles using the phage M13 gene 5 protein (g5p) as the molecular glue to bind two antiparallel noncomplementary ssDNA strands. The entire process was controlled tightly by the concentration of the g5p protein and the presence of double-stranded DNA. The g5p−ssDNA aggregate was disintegrated by hybridization with complementary ssDNA (C-ssDNA) that triggers the dissociation of the complex. Polyhistidine-tagged g5p was bound to nickel nitrilotriacetic acid (Ni^{2+}-NTA) conjugated nanoparticles and subsequently used to coassemble the ssDNA-conjugated nanoparticles into multiparticle-type aggregates. Our approach offers great promise for designing biologically functional, controllable protein/nanoparticle composites.

Introduction

The remarkable specificity and programmable interactions of DNA support the self-assembly of DNA-conjugated nanoparticles (DNA-nanoparticles)[1−8] and the construction of complex architectures.[9−11] Further, we can extend the complexity and functionality of such DNA-based nanosystems by incorporating proteins having enzymatic and binding functions with high specificity and selectivity.[12−14]

Filamentous bacteriophages such as M13 encode the gene 5 protein (g5p) that cooperatively binds to single-stranded DNA (ssDNA) to form precursors for assembling phage particles. *In vitro*, g5p forms a homodimer that nonspecifically binds two antiparallel ssDNAs, inducing helical rodlike structures with an 8−9 nm outer diameter.[15,16] The number of nucleotides bound to a g5p monomer (binding mode, referred to as "*n*") can be 2−4, depending upon the binding conditions including the protein-to-nucleotide ratio.[17] The binding affinity of g5p to ssDNA, that is, $\sim 10^5$ to $\sim 10^6$ M^{-1}, rests on the sequence of ssDNA and the salt concentration,[18,19] with preferential binding to structured DNA, such as hairpins[20] and G-quadruplexes.[21]

Efficient linkage between DNA and proteins is crucial to add protein functionality to DNA-based nanosystems. We therefore suggest using DNA binding proteins, such as g5p, as this would allow extending the complexity and functionality of the systems while excluding the further need for chemical modification of DNA or proteins. We present a method for the controllable assembly and disassembly of DNA-conjugated nanoparticles wherein we employed g5p as the molecular glue to bind two antiparallel noncomplementary ssDNA strands. The inherent temperature-dependence of DNA hybridization and denaturation could limit the incorporation of temperature-sensitive biological molecules, including proteins, into hybrid nanomaterials. However, hybridization with complementary ssDNA (C-ssDNA), which triggers the dissociation of the g5p−ssDNA complex, enables us to control both the assembly and disassembly of nanoparticle aggregates at room temperature (Scheme 1). With further genetic engineering of g5p, it can be used to confer biological functionality on the nanoparticle aggregates. To demonstrate this approach, we employed polyhistidine-tagged g5p to coassemble nickel nitrilotriacetic acid (Ni^{2+}-NTA) conjugated nanoparticles with ssDNA-conjugated nanoparticles into multiparticle-type aggregates. Our concept offers great opportunities to design biologically active protein/nanoparticle composites with controllable assembly properties.

Experimental Section

Protein Preparation. The g5p gene of bacteriophage M13 (New England Biolabs (NEB)) was PCR- amplified using the primers 5′-TAATTC**CATATG**ATTAAAGTTGAAATTAAACCA-3′ and

* To whom correspondence should be addressed. Telephone: 1-631-344-5349. Fax: 1-631-344-3407. E-mail: vdlelied@bnl.gov. Address: Biology Department, Brookhaven National Laboratory, Upton, NY 11973.

† Center for Functional Nanomaterials.

‡ Biology Department.

(1) Alivisatos, A. P.; Johnsson, K. P.; Peng, X. G.; Wilson, T. E.; Loweth, C. J.; Bruchez, M. P.; Schultz, P. G. *Nature* **1996**, *382*(6592), 609–611.

(2) Mirkin, C. A.; Letsinger, R. L.; Mucic, R. C.; Storhoff, J. J. *Nature* **1996**, *382*(6592), 607–609.

(3) Elghanian, R.; Storhoff, J. J.; Mucic, R. C.; Letsinger, R. L.; Mirkin, C. A. *Science* **1997**, *277*(5329), 1078–1081.

(4) Taton, T. A.; Mirkin, C. A.; Letsinger, R. L. *Science* **2000**, *289*(5485), 1757–1760.

(5) He, L.; Musick, M. D.; Nicewarner, S. R.; Salinas, F. G.; Benkovic, S. J.; Natan, M. J.; Keating, C. D. *J. Am. Chem. Soc.* **2000**, *122*(38), 9071–9077.

(6) Taton, T. A.; Lu, G.; Mirkin, C. A. *J. Am. Chem. Soc.* **2001**, *123*(21), 5164–5165.

(7) Park, S. J.; Taton, T. A.; Mirkin, C. A. *Science* **2002**, *295*(5559), 1503–1506.

(8) Stoermer, R. L.; Cederquist, K. B.; McFarland, S. K.; Sha, M. Y.; Penn, S. G.; Keating, C. D. *J. Am. Chem. Soc.* **2006**, *128*(51), 16892–16903.

(9) Mao, C. D.; Sun, W. Q.; Shen, Z. Y.; Seeman, N. C. *Nature* **1999**, *397*(6715), 144–146.

(10) Yan, H.; Zhang, X. P.; Shen, Z. Y.; Seeman, N. C. *Nature* **2002**, *415*(6867), 62–65.

(11) Bath, J.; Turberfield, A. J. *Nat. Nanotechnol.* **2007**, *2*(5), 275–284.

(12) Nam, J. M.; Park, S. J.; Mirkin, C. A. *J. Am. Chem. Soc.* **2002**, *124*(15), 3820–3821.

(13) Niemeyer, C. M.; Adler, M.; Pignataro, B.; Lenhert, S.; Gao, S.; Chi, L. F.; Fuchs, H.; Blohm, D. *Nucleic Acids Res.* **1999**, *27*(23), 4553–4561.

(14) Niemeyer, C. M.; Koehler, J.; Wuerdemann, C. *ChemBioChem* **2002**, *3*(2−3), 242–245.

(15) Olah, G. A.; Gray, D. M.; Gray, C. W.; Kergil, D. L.; Sosnick, T. R.; Mark, B. L.; Vaughan, M. R.; Trewhella, J. *J. Mol. Biol.* **1995**, *249*(3), 576–594.

(16) Folmer, R. H. A.; Nilges, M.; Folkers, P. J. M.; Konings, R. N. H.; Hilbers, C. W. *J. Mol. Biol.* **1994**, *240*(4), 341–357.

(17) Thompson, T. M.; Mark, B. L.; Gray, C. W.; Terwilliger, T. C.; Sreerama, N.; Woody, R. W.; Gray, D. M. *Biochemistry* **1998**, *37*(20), 7463–7477.

(18) Terwilliger, T. C. *Biochemistry* **1996**, *35*(51), 16652–16664.

(19) Mou, T. C.; Gray, C. W.; Gray, D. M. *Biophys. J.* **1999**, *76*(3), 1537–1551.

(20) Wen, J. D.; Gray, D. M. *Biochemistry* **2004**, *43*(9), 2622–2634.

(21) Wen, J. D.; Gray, D. M. *Biochemistry* **2002**, *41*(38), 11438–11448.

10.1021/la803596q CCC: $40.75
Published on Web 12/12/2008

Scheme 1. g5p-Directed Assembly and DNA-Controlled Disassembly of ssDNA-Conjugated Nanoparticles[a]

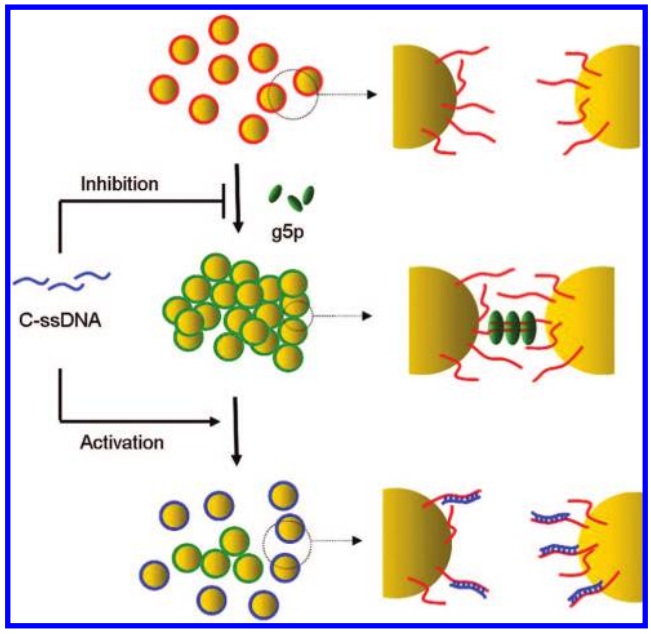

[a] Adding complementary ssDNA (C-ssDNA) inhibits the g5p-directed assembly and causes dissociation of g5p by hybridization of C-ssDNA.

5′-TAGCTT**GCTCTTC**CGCACTTAGCCGGAACGAGGCG-3′. This procedure generates a DNA fragment flanked by *NdeI* and *SapI* restriction sites (bold letters). The polymerase chain reaction (PCR) product was digested with *NdeI* and *SapI* (NEB) and ligated into the pET-30b vector (Novagen). After confirming the sequence, we introduced the recombinant plasmid into BL21-DE3 electroporation competent cells, using the Gene Pulser Xcell system (Bio-Rad). The g5p-His expression was induced by adding isopropyl *β-D*-1-thiogalactopyranoside (IPTG) (Sigma) in lysogeny broth (LB) medium with kanamycin (100 μg/mL) (Sigma). After a 6 h expression period, the cells were sonicated, and the g5p-His purified on a Ni-NTA column (Qiagen). We further purified g5p-His by fast protein liquid chromatography (FPLC) (AKTA explorer, GE Healthcare) with a Sephacryl S-200 high-resolution sizing column (Amersham Biosciences). A purity of >95% was obtained, as determined by analyzing the protein bands using Quantity One software (Bio-Rad), after staining with Coomassie Blue on a 15% SDS-polyacrylamide gel. A molar extinction coefficient of 7450 M^{-1} cm^{-1} was used to assess the protein concentration. The YieF (from *E. coli*) protein was prepared as we described previously.[22]

Characterization. UV−visible spectra were obtained using a PerkinElmer Lambda 35 spectrometer. Dynamic light scattering (DLS) was measured using the Malvern Zetasizer ZS instrument equipped with a 633 nm laser and a backscattering detector at 173°. To visualize ssDNA-Au, we operated the JEOL 1300 TEM at 120 kV. We prepared the transmission electron microscopy (TEM) samples by incubating them on a carbon-coated copper grid for 10 min and then washing them twice with distilled water. We carried out our small angle X-ray scattering (SAXS) experiments at the National Synchrotron Light Source's X-21 beamline. The scattering data were collected with a MAR CCD area detector at wavelength λ = 1.5498 Å. We present these data as the structure factor S(q) versus scattering vector, $q = (4\pi/\lambda)\sin(\theta/2)$, where θ is the scattering angle. The values of q were calibrated with silver behenate (q = 0.1076 $Å^{-1}$). S(q) was calculated as $I_a(q)/I_p(q)$, where $I_a(q)$ and $I_p(q)$ are, respectively, the background-corrected angular-averaged 1D scattering intensities for the system under consideration and unaggregated system. The peak positions in $S(q)$ were determined by fitting a Lorenzian form.

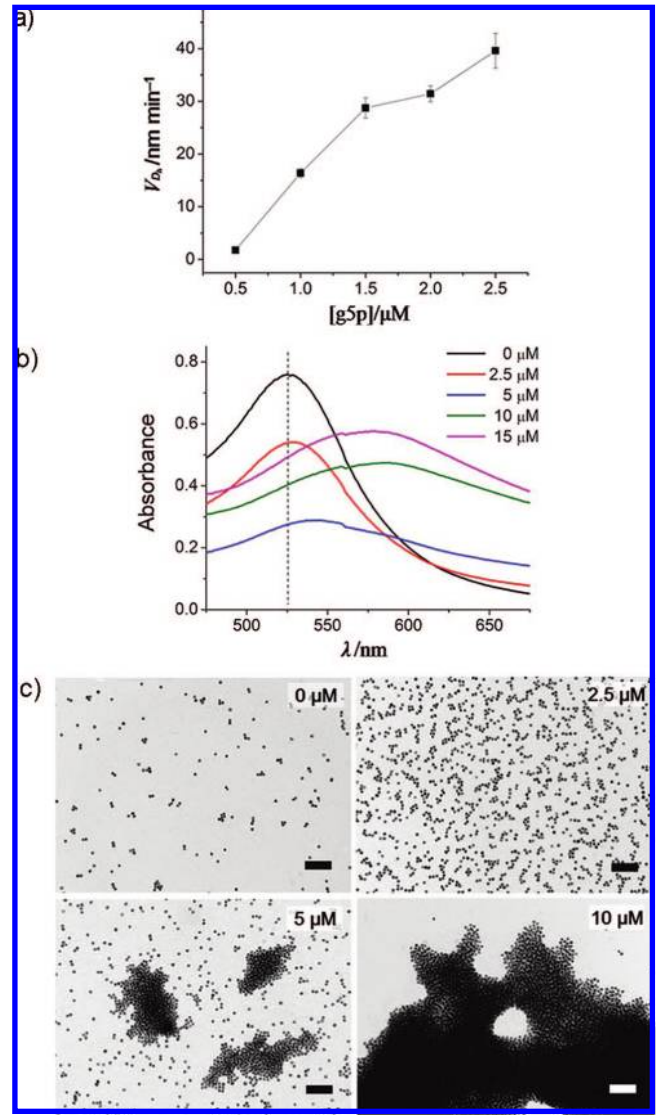

Figure 1. G5p-His-directed assembly of ssDNA-conjugated gold particles (ssDNA-Au). (a) Results of dynamic light scattering showing initial rate of hydrodynamic diameter value (D_h) during incubation of ssDNA-Au (5 nM) and g5p-His. (b) UV−vis spectra of aggregates after ~24 h incubation of ssDNA-Au (20 nM) with g5p-His (at concentrations of 0, 2.5, 5, 10, and 15 μM in 10 mM Tris-HCl, pH 7.4, 200 mM NaCl). (c) Transmission electron microscope images of (b). Scale bars in (c) are 100 nm.

Results and Discussion

To exploit g5p's ability for assembling ssDNA-conjugated nanoparticles (ssDNA-Au), we synthesized gold nanoparticles (Au) that were surface covered with approximately 50 copies of ssDNA (5′-HS-C3H6-(T)15-TAACCTAACCTTCAT-3′),[23] to which we added purified polyhistidine-tagged g5p (g5p-His). With DLS, we measured changes in the value of the hydrodynamic diameter (D_h) that is related to the aggregate's size, interparticle interactions, and geometry. Figure 1a shows that the initial assembly rate of D_h during a 20 min incubation of the ssDNA-Au nanoparticles and g5p-His was highly sensitive to the latter's concentration, indicating the g5p-His-dependent assembly of ssDNA-Au. No assemblage was observed in its absence. To investigate the assembly of ssDNA-Au (20 nM) during prolonged incubations (~24 h) with a series of g5p-His concentrations, we

(22) Zhang, Y. B.; Kanungo, M.; Ho, A. J.; Freimuh, P.; Lelie, D. V. D.; Chen, M.; Khamis, S. M.; Datta, S. S.; Johnson, A. T. C.; Misewich, J. A.; Wong, S. S. *Nano Lett.* **2007**, *7*(10), 3086–3091.

(23) Maye, M. M.; Nykypanchuk, D.; van der Lelie, D.; Gang, O. *J. Am. Chem. Soc.* **2006**, *128*(43), 14020–14021.

recorded the ssDNA-Au surface plasmon (SP) resonance band by UV−visible spectrophotometry (UV−vis). The SP band is associated with isolated Au and assembled nanostructures. After increasing g5p-His concentrations, the SP band at 525 nm, characteristic of isolated ssDNA-Au, was red-shifted with band broadening (Figure 1b), indicative of either a decrease in interparticle distances or an increase in aggregate size.[24] The higher extinction intensity observed over 10 μM g5p-His reflects the decline in the solution's turbidity resulting from the formation of larger aggregates.[25] Both the DLS and UV−vis results confirmed that the assembly of ssDNA-Au was mediated by g5p-His. The sizes and morphologies of these conglomerates were studied using TEM (Figure 1c). The aggregates' sizes increased with rising g5p-His concentrations, as suggested by the DLS and UV−vis findings, while the numbers of non-assembled particles decreased, implying that the size of aggregates can be controlled simply by the g5p-His concentration.

We employed SAXS with synchrotron radiation, which supports *in situ* investigations of the samples in their native buffer environment, to evaluate the interparticle distances (d) of the aggregates; the data revealed that d was, respectively, ∼9.3, ∼9.2, and ∼9.7 nm with 5, 7.5, and 10 μM g5p-His (see the Supporting Information, Figure S1). In contrast, the estimated d from a model approximation based on length of the g5p-His complex with 30 bases long ssDNA (g5p binding mode of n = 3 or 4) ranges from ∼7.2 to ∼8.2. The higher d values observed could be due to limited g5p-His binding to the base of the ssDNA at the gold's surface. At higher g5p-His concentrations (20 μM), d increased to ∼11.2 nm, suggesting a change of binding mode to $n \approx 2-2.5$ that entails an increase in the length of the g5p-His complex.[17] Polyhistidine-tagged YieF protein (MW = 20 KDa) was used as a negative control; no aggregation of particles was observed during DLS and UV−vis studies (see the Supporting Information, Figure S2). These results clearly illustrate the value of g5p-His for ensuring the controlled assembly of ssDNA-Au by changing the protein−nanoparticle ratios.

To investigate inhibitory effects of dsDNA on aggregate formation, the ssDNA-capping of the particles first was partially hybridized with complementary ssDNA (C-ssDNA, 5′-ATGAAGGTTAGGTTA-3′) before initiating the g5p-His-mediated assembly. We recorded changes in the assembly rate in response to C-ssDNA concentrations using DLS (Figure 2). The assembly rate dramatically dropped when the fraction of C-ssDNA to ssDNA on Au (f_c) was above $n \sim 0.05$. This large inhibition caused by a low density of dsDNA points to considerable steric hindrance to the binding of g5p-His for assembling ssDNA-Au. As a control, we used noncomplementary ssDNA (NC-ssDNA; 5′-AATATTGATAAGGATAGC-3′) to eliminate any inhibitory titration effects caused by the binding of g5p-His to ssDNA in solution. The effect of the NC-ssDNA on the assembly rate was statistically insignificant (Figure 2).

C-ssDNA hybridization can replace the binding of g5p to ssDNA and so should result in the dissociation of the aggregates. To prove this, we prepared aggregates by incubating ssDNA-Au (10 nM) and g5p-His (5 μM) for ∼24 h and then incubated them with C-ssDNA for ∼12 h at room temperature. Colorimetric changes, reflecting changes in aggregate size, were monitored using UV−vis. The peak position blue-shifted at concentrations of over ∼200 nM C-ssDNA (f_c = ∼0.4) (Figure 3a), indicating the dissociation of small clusters and release of individual particles. In the NC-ssDNA control, the peak intensity slightly

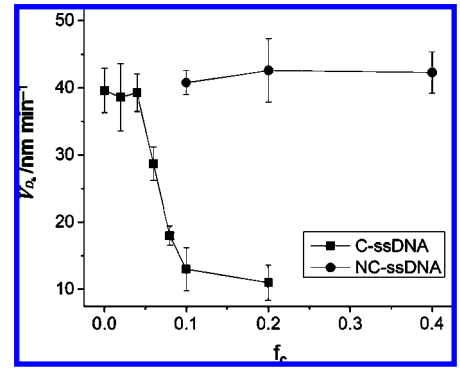

Figure 2. Inhibition of g5p-His-directed assembly of ssDNA-conjugated gold particles (ssDNA-Au) by hybridization with complementary ssDNA (C-ssDNA). Initial rate of hydrodynamic diameter (D_h) during g5p-His (2.5 μM)-directed assembly of ssDNA-Au (5 nM), which was prehybridized with C-ssDNA or noncomplementary ssDNA (NC-ssDNA) (f_c = number of C-ssDNA/number of ssDNA on gold nanoparticles).

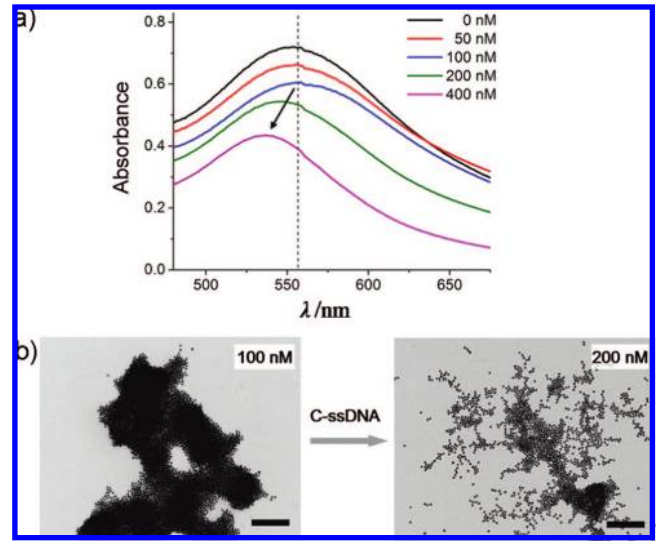

Figure 3. Decomposition of g5p-His-directed ssDNA-conjugated gold particle (ssDNA-Au) aggregates by adding complementary ssDNA (C-ssDNA). (a) UV−vis spectra of the aggregates (10 nM ssDNA-Au and 5 μM g5p-His) after ∼12 h incubation with C-ssDNA (0, 50, 100, 200, and 400 nM). The arrow indicates a shift in peak position. (b) Transmission electron microscope images of the samples after incubation with 100 nM (f_c = ∼0.2) and 200 nM C-ssDNA (f_c = ∼0.4). Scale bars in (b) are 200 nm.

decreased but there was no shift in peak position (see the Supporting Information, Figure S3); thus, NC-ssDNA could disrupt the aggregates into smaller clusters, but not to the level of individual particles. The TEM image of the sample with 200 nM C-ssDNA clearly shows this dissociation into dispersed particles (Figure 3b), whereas it was not observed in the sample with NC-ssDNA.

Peptides have been used successfully for the construction of nanostructures[26] and the self-assembly of inorganic nanoparticles.[27−29] The well-known ability of the polyhistidine tag to bind to Ni^{2+}-NTA is a useful tool for targeting proteins to inorganic

(24) Storhoff, J. J.; Lazarides, A. A.; Mucic, R. C.; Mirkin, C. A.; Letsinger, R. L.; Schatz, G. C. *J. Am. Chem. Soc.* **2000**, *122*(19), 4640–4650.
(25) Elimelech, M.; Gregory, J.; Jia, X.; Williams, R. A. *Particle Deposition & Aggregation*; Butterworth-Heinemann: Boston, MA, 1995; p 268−272.
(26) Gao, X. Y.; Matsui, H. *Adv. Mater.* **2005**, *17*(17), 2037–2050.
(27) Whaley, S. R.; English, D. S.; Hu, E. L.; Barbara, P. F.; Belcher, A. M. *Nature* **2000**, *405*(6787), 665–668.
(28) Lee, S. W.; Mao, C. B.; Flynn, C. E.; Belcher, A. M. *Science* **2002**, *296*(5569), 892–895.
(29) Sarikaya, M.; Tamerler, C.; Jen, A. K. Y.; Schulten, K.; Baneyx, F. *Nat. Mater.* **2003**, *2*(9), 577–585.

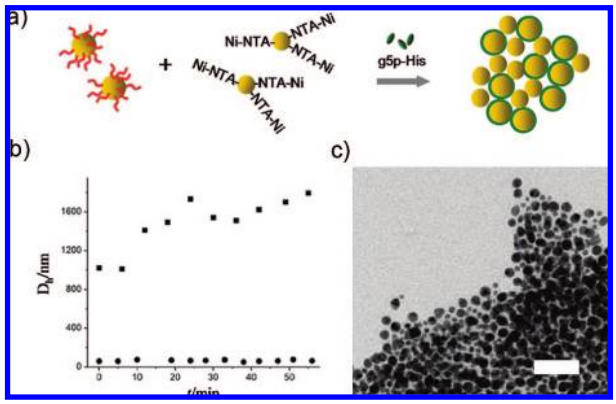

Figure 4. (a) Schematic diagram illustrating the aggregation of ssDNA-conjugated gold particles (ssDNA-Au) and Ni-NTA-conjugated gold particles (Ni-NTA-Au) by the binding of g5p-His to both ssDNA and Ni-NTA. (b) Results of dynamic light scattering during incubation of ssDNA-conjugated gold particles (ssDNA-Au) (2 nM) and Ni-NTA-conjugated gold particles (Ni-NTA-Au) (10 nM) in the presence (■) and absence (●) of g5p-His (1 μM). (c) Transmission electron microscope image of the aggregates after incubating ssDNA-Au (10 nM) and Ni-NTA-Au (40 nM) with g5p-His (5 μM) for ∼24 h. Scale bar in (c) is 50 nm.

surfaces.[30] We used g5p-His to induce the assembly of both ssDNA-Au- (diameter = ∼12 nm) and Ni-NTA-conjugated gold nanoparticles (diameter = ∼4 nm) (Ni-NTA-Au) into multi-particle-type aggregates (Figure 4a). DLS data support the aggregation of ssDNA-Au (2 nM) and Ni-NTA-Au (10 nM) with g5p-His (1 μM); aggregates were not observed without the presence of g5p-His (Figure 4b). The TEM image of the aggregates (Figure 4c) shows well-distributed Ni-NTA-Au among ssDNA-Au, meaning that co-aggregation occurs by the binding of g5p-His to DNA and Ni-NTA.

(30) Hainfeld, J. F.; Liu, W. Q.; Halsey, C. M. R.; Freimuth, P.; Powell, R. D. *J. Struct. Biol.* **1999**, *127*(2), 185–198.

Conclusion

In this Letter, we describe a new method for controllable aggregation and dissociation of DNA-conjugated nanoparticle composites using the g5p-His protein as the driving force. The kinetics of assembly and dissociation of particle aggregates can be controlled via sequence-specific hybridization with C-ssDNA, while the size of aggregates is modulated by adjusting the g5p-His concentration. We demonstrated the coassembly of Ni^{2+}-NTA-conjugated nanoparticles and ss-DNA-conjugated gold particles by adding polyhistidine-tagged g5p protein. Further, genetic engineering of g5p, for example, via linkage to other affinity tags, might well afford opportunities to construct more sophisticated, biologically functional nanostructures. We also note that this new assembly approach, based on g5p, ssDNA, and affinity tags, can be extended to other kinds of nanomaterials, such as carbon nanotubes, semiconductors, and magnetic nanoparticles.

Acknowledgment. This work was supported by the U.S. DOE Office of Science and Office of Basic Energy Sciences under Contract No. DE-AC-02-98CH10886. We would like to express our thanks to Avril Woodhead for commenting this manuscript.

Supporting Information Available: Synthesis method of Ni-NTA-conjugated gold nanoparticles; small angle X-ray scattering results of g5p protein-mediated assembly of ss-DNA-conjugated gold particles; dynamic light scattering and UV−visible spectrophotometry of ss-DNA-conjugated gold particles in the presence of the g5p-His or YieF proteins; and UV−visible spectra of the aggregates (10 nM ssDNA-Au and 5 μM g5p-His) after ∼12 h incubation with NC-ssDNA. This material is available free of charge via the Internet at http://pubs.acs.org.

LA803596Q